Inverse Scattering Algorithm for Reconstructing Strongly Reflecting Fiber Bragg Gratings

Amir Rosenthal and Moshe Horowitz

***Abstract*—We demonstrate a new inverse scattering algorithm for reconstructing the structure of highly reflecting fiber Bragg gratings. The method, called integral layer-peeling (ILP), is based on solving the Gel'fand-Levitan-Marchenko (GLM) integral equation in a layer-peeling procedure. Unlike in previously published layer-peeling algorithms, the structure of each layer in the ILP algorithm can have a nonuniform profile. Moreover, errors due to the limited bandwidth used to sample the reflection coefficient do not rapidly accumulate along the grating. Therefore, the error in the new algorithm is smaller than in previous layer peeling algorithms. The ILP algorithm is compared to two discrete layer-peeling algorithms and to an iterative solution to the GLM equation. The comparison shows that the ILP algorithm enables to solve numerically difficult inverse scattering problems, where previous algorithms failed to give an accurate result. The complexity of the ILP algorithm is on the same order as in previous layer peeling algorithms. When a small error is acceptable, the complexity of the ILP algorithm can be significantly reduced below the complexity of previously published layer-peeling algorithms.**

***Index Terms*—Gratings, inverse problems, optical fiber devices, periodic structures.**

I. Introduction

FIBER BRAGG gratings are important for various applications in optical communication systems and in systems for optical metrology. When the grating structure is known, the complex reflection spectrum of the grating can be calculated numerically [1], [2]. The problem of calculating the spectrum from the grating profile is often referred to as a direct scattering problem. However, in several important applications, the structure of a grating should be found from its complex reflection spectrum. In a reconstruction problem, the grating reflection spectrum is measured experimentally in order to extract the grating profile [3], [4]. In a synthesis problem, the grating profile is extracted from the desired spectral response [5]–[11]. The problem of calculating the grating profile from its complex reflection spectrum is often referred to as an inverse scattering problem.

Several methods for solving the inverse scattering problem in fiber Bragg gratings have been demonstrated [5]–[11]. The first type of solution is based on solving the GLM integral equation. The solution to the GLM equation is unique, and can be used to extract the grating profile [12]. An analytical solution to the GLM equation is obtained when the grating reflection spectrum can be expressed as a rational function [5]. An iterative solution can be used to solve the GLM equation for a more general reflection spectrum [6]–[8]. One of the methods that can be easily applied is based on calculating a series of successive integrals in order to estimate the kernel functions [7], [8]. The order of the integrals is proportional to the number of iterations. Although the iterative solution gives an accurate result for gratings with a moderate reflectivity, its complexity is high and is equal to $O(N^3)$ [9], where N is the number of points in the grating. When the grating reflectivity is high, many iterations are needed to obtain an accurate result. Since the reflection spectrum is sampled with a limited bandwidth and resolution, the high-order integrals can not be calculated accurately. Therefore, the error of the iterative solution does not vanish for highly reflecting gratings, even when the number of iterations is increased.

A newer approach for solving the inverse scattering problem is the differential inverse scattering method, also referred to as layer-peeling. This method was generalized by Bruckstein *et al.* [13] for solving various inverse scattering problems. The layer-peeling method is based on causality principle: the front edge of the impulse response is proportional to the structure at the beginning of the grating. In layer-peeling algorithms, the grating is divided into thin layers, each assumed to have a uniform profile. The structure of the first layer can be determined directly from the impulse response. The extracted grating profile of the first layer is used to calculate the fields at the beginning of the next layer, using a solution to the direct scattering problem. The process is repeated until the whole grating structure is revealed.

The layer-peeling method was implemented using a continuous [10] or a discrete [9], [11] model of the grating. In the discrete model, the grating is presented by a limited number of point reflectors. There are three main implementations to the discrete layer peeling (DLP) algorithm described in [9], [11]. The DLP algorithm can be implemented in the time domain (TDLP) [11], in the frequency domain (FDLP) [11], or in both the frequency and time domain (FTDLP) [9]. The FTDLP is based on an extensive use of the fast Fourier transform (FFT). This algorithm is usually more robust but significantly slower than the FDLP algorithm. The complexity of layer-peeling algorithms is equal to $O(N^2\log(N))$ or $O(N^2)$, compared to $O(N^3)$ of the iterative solution to the GLM equation. In a recently published paper, Skaar *et al.* [11] compared the discrete and continuous implementations, and found out that the FDLP algorithm is significantly faster and is often more stable, while the continuous layer-peeling (CLP) algorithm offers some advantages in flexibility. When both the FDLP and

Manuscript received November 6, 2002; revised February 26, 2003. This work was supported by the Division for Research Funds of the Israeli Ministry of Science.

The authors are with the Department of Electrical Engineering, Technion—Israel Institute of Technology, Haifa 32000, Israel (e-mail: eeamir@tx.technion.ac.il; horowitz@ee.technion.ac.il).

Digital Object Identifier 10.1109/JQE.2003.814365

CLP algorithms are stable, the accuracy of the two algorithms is approximately the same [11]. The limited bandwidth and resolution of the reflection coefficient is the main source of error in layer-peeling algorithms. The error accumulates along the grating through the peeling process. The DLP and CLP algorithms enable to accurately reconstruct most of the practical gratings. However, when the grating reflectivity is very high, the error may become significant and may prevent an accurate reconstruction of the grating profile. Moreover, the reconstruction accuracy of such gratings strongly depends on the bandwidth used to present the reflection coefficient.

In this paper, we demonstrate a new layer-peeling algorithm called integral layer-peeling (ILP). The algorithm is based on solving the GLM integral equation in a layer-peeling procedure. The grating is divided into several layers. Unlike in previous layer-peeling algorithms, each layer in the ILP algorithm may have a nonuniform profile. The GLM equation is solved for each layer, in order to find the complex reflection coefficient of the next layer, and in order to extract the layer profile. In contrary to former layer-peeling methods, errors due to the limited bandwidth used to sample the reflection coefficient, do not rapidly accumulate along the grating. Hence, the total error of the ILP algorithm is smaller than obtained in former layer-peeling algorithms. The high accuracy of the ILP algorithm is achieved with the same complexity as in former layer-peeling algorithms. The ILP algorithm is extremely stable, and could be used to solve numerically difficult problems, where previous algorithms [8]–[11] failed to give an accurate result using the same bandwidth and spectral resolution. The algorithm enabled to analyze even a uniform grating with an extremely high maximum reflectivity of $1-10^{-10}=0.999\,999\,999\,9$. When a slight inaccuracy is acceptable, the complexity of the algorithm can be significantly reduced below the complexity of former layer-peeling algorithms. The dependence of the result accuracy of the ILP algorithm on the bandwidth used to present the reflection spectrum is significantly smaller than in previous algorithms. This advantage becomes especially important in the reconstruction of highly reflecting gratings from measurements [4].

II. Theoretical Background

The refractive index profile of a fiber Bragg grating $n(z)$ can be modeled as [2], [5]

$$n(z)=n_{\rm avg}+n_0(z)+n_1(z)\sin\left[\frac{2\pi}{\Lambda}z+\theta(z)\right] \tag{1}$$

where $n_{\rm avg}$ is the average refractive index, $n_0(z)$ is the spatially dependent average refractive index, $n_1(z)$ is the amplitude of the refractive index modulation, and Λ is the average grating period. When absorption effect can be neglected, the propagation of an optical wave with a wavenumber β can be modeled by the coupled mode equations [2], [5]

$$\begin{aligned}\frac{du_1(k,z)}{dz}+iku_1(k,z)&=q(z)u_2(k,z)\\ \frac{du_2(k,z)}{dz}-iku_2(k,z)&=q^*(z)u_1(k,z)\end{aligned} \tag{2}$$

where $k=\beta-\pi/\Lambda$ is the wavenumber detuning, $u_1(k,z)$ and $u_2(k,z)$ are the complex amplitudes of the backward- and forward-propagating waves respectively, and $q(z)$ is the complex coupling coefficient of the grating, defined as

$$q(z)=\frac{\pi}{2n_{\rm avg}\Lambda}n_1(z)\exp\left[-i\theta(z)+i\frac{2\pi}{n_{\rm avg}\Lambda}\int_0^z n_0(z')dz'\right]. \tag{3}$$

We assume that the gratings is written in the region [0, L]. Note that when the coupling coefficient $q(z)$ is given, the separation between the average refractive index $n_0(z)$ and the phase $\theta(z)$ cannot be uniquely determined.

In the direct scattering problem, (2) is solved for given coupling coefficient and boundary conditions. The solution can be found by dividing the grating into narrow uniform sections. The transfer matrix of each section can be found using an analytical solution [1], [2]. The transfer matrix of the whole grating is obtained by multiplying the transfer matrices of all the sections. Assuming that the boundary conditions are $u_1(k,z=L)=0$ and $u_2(k,z=0)=f(k)$, the reflection coefficient of the grating $r(k)=u_1(k,z=0)/u_2(k,z=0)$ can be calculated. Note that since the problem is linear, the reflection coefficient does not depend on the boundary condition $u_2(k,z=0)$. The complex reflection spectrum is often used to characterize gratings, since it can be measured experimentally [3], [15]. It is possible to present the fields in the time domain using a Fourier transform $u_{1,2}(\tau,z)=(1/2\pi)\int_{-\infty}^{\infty}u_{1,2}(k,z)\exp(-ik\tau)dk$, where $\tau=ct/n_{\rm avg}$ is normalized time, c is the velocity of light in vacuum, and t is time. The impulse response of the grating is equal to the Fourier transform of the complex reflection coefficient

$$h(\tau)=\frac{1}{2\pi}\int_{-\infty}^{\infty}r(k)\exp(-ik\tau)dk. \tag{4}$$

Inverse scattering methods are used to calculate the grating profile $q(z)$ from the complex reflection coefficient $r(k)$. When the grating profile $q(z)$ obeys $\int_{-\infty}^{\infty}|q(z)|z^m\,dz<\infty$ for every integer number m, the complex reflection spectrum defines a unique solution to the inverse scattering problem [12]. Therefore, when the grating length is finite, there is always a unique solution to the inverse scattering problem. There are two main approaches to solve inverse scattering problems in fiber Bragg gratings. The first, called layer-peeling, is based on a method generalized by Bruckstein *et al.* [13]. The layer-peeling algorithm uses the known solution to the direct scattering problem in order to solve the inverse scattering problem. The grating is divided into thin layers, each assumed to have a uniform profile. The coupling coefficient of the first layer is proportional to the front edge of the impulse response, due to causality principle. Therefore, the coupling coefficient of the first layer can be extracted directly from the reflection coefficient by substituting $\tau=0$ in (4). The extracted coupling coefficient of the first layer is used to find the reflection coefficient of the second layer, using a direct solution to the coupled-mode equations [(2)]. Then, the procedure is repeated until the structure of the whole grating is revealed. The main advantages of the layer-peeling algorithm are its simplicity and low complexity, that are compared to the solution of the direct problem [10].

Several different layer-peeling algorithms have been demonstrated [9]–[11] and can accurately reconstruct most of the practical gratings. However, when the algorithms are used to solve numerically difficult inverse scattering problems, such as reconstructing gratings with a very high reflectivity, the error may become significant and may prevent an accurate reconstruction of the grating profile. The inaccuracies in layer-peeling algorithms are mainly caused by the numerical calculation of (4), using a FFT with a finite bandwidth and spectral resolution [16]. In a practical problem, the bandwidth and the resolution used to present the reflection spectrum are limited. When the grating profile is reconstructed from experimental measurements, the resolution and the bandwidth are limited by the experimental setup. When a grating is synthesized, the resolution and bandwidth are limited by calculation runtime. The inaccuracy in calculating FFT causes an error in calculating the grating profile and in propagating the fields along the grating. The numerical error in propagating the fields accumulates through the peeling procedure. Another source of error in layer-peeling algorithms is the assumption that each layer has a uniform structure or formed by a discrete reflector. The error in extracting the grating profile becomes significant in gratings with a very high reflectivity. In a highly reflecting grating, the forward-propagating wave rapidly decays along the grating. Therefore, the section of the grating, located close to the output end, does not significantly affect the reflection coefficient of the whole grating [4]. Since the intensity of the transmitted wave rapidly decays along a highly reflecting grating, the accumulated error may become on the same order as the reflection from the region, located near the output end of the grating.

The second approach for solving the inverse scattering problem in fiber Bragg gratings is based on a solution to the GLM integral equation [12]. Since our approach requires solving the GLM equation, in the following, we give a short theoretical background on the subject.

We use a vectorial notation to present the inverse scattering problem $\mathbf{u}(k,z) = (u_1(k,z), u_2(k,z))$, where $u_1(k,z)$, $u_2(k,z)$ are the solutions to coupled-mode equations [(2)] with the boundary conditions $u_1(k, z = L) = 0$ and $u_2(k, z = 0) = 1$. Since coupled-mode equations are linear, the solution $\mathbf{u}(k,z)$ can be written as sum of two independent solutions $\mathbf{\Phi}(k,z)$, $\overline{\mathbf{\Phi}}(k,z)$ with the boundary conditions: $\mathbf{\Phi}(k, z \to -\infty) = (\exp[-ikz], 0)$ and $\overline{\mathbf{\Phi}}(k, z \to -\infty) = (0, \exp[ikz])$] [12]. Since $\mathbf{u}(k,0) = (r(k), 1)$, we obtain

$$\mathbf{u}(k,z) = \overline{\mathbf{\Phi}}(k,z) + r(k)\mathbf{\Phi}(k,z). \tag{5}$$

Using the symmetry properties of (2), it can be shown that $\overline{\mathbf{\Phi}}(k,z) = (\Phi_2^*(k,z), \Phi_1^*(k,z))$, where $\Phi_{1,2}(k,z)$ are the vector components of $\mathbf{\Phi}(k,z)$ [12]. The vector $\overline{\mathbf{\Phi}}(k,z)$ can be represented as [12]

$$\overline{\mathbf{\Phi}}(k,z) = \begin{bmatrix} 0 \\ 1 \end{bmatrix} \exp(ikz) + \int_{-\infty}^{z} \begin{bmatrix} A_1(\tau,z) \\ A_2(\tau,z) \end{bmatrix} e^{ik\tau} d\tau \tag{6}$$

where $\mathbf{A}(\tau,z) = (A_1(\tau,z), A_2(\tau,z))$, are the kernel functions, that give the difference between the solution, $\overline{\mathbf{\Phi}}(k,z)$, and the boundary value at $z = -\infty$. By substituting (6) into (5) and performing a Fourier transform, the GLM integral equation is obtained as follows:

$$\mathbf{A}(\tau,z) + \begin{bmatrix} 1 \\ 0 \end{bmatrix} h(z+\tau) + \int_{-\infty}^{z} \begin{bmatrix} A_2^*(y,z) \\ A_1^*(y,z) \end{bmatrix} h(y+\tau)dy = 0, \quad \tau < z. \tag{7}$$

In deriving (7), we used the causality of the problem $\mathbf{u}(\tau,z) = 0$ for $\tau < z$.

After the kernel functions $\mathbf{A}(\tau,z)$ are calculated, the profile of the grating can be found by substituting (6) into (2)[12]

$$q(z) = 2A_1(z,z). \tag{8}$$

The refractive index profile of the grating can be found from the coupling coefficient $q(z)$ using (3). The fields inside the grating $\mathbf{u}(k,z)$ can be found from the kernel functions using (5) and (6).

The zero-order solution to (7), often referred to as the Born approximation, is obtained by neglecting the integral terms in (7)

$$\mathbf{A}(\tau,z) = -\begin{bmatrix} 1 \\ 0 \end{bmatrix} h(z+\tau) \quad \tau < z. \tag{9}$$

The Born approximation is accurate when multiple reflections inside the grating are negligible. Multiple reflections can be neglected in gratings with a weak reflectivity or at the beginning of highly reflecting gratings ($z \approx 0$). Therefore, the profile close to the input end of a grating can be extracted by substituting (9) into (8)

$$q(z) = -2h(2z). \tag{10}$$

When multiple reflections can not be neglected, an iterative solution to the GLM equation can be used [7], [8]. The zero-order solution of the iterative algorithm is given by the Born approximation [(9)]. The solution of iteration $i+1$ ($i \geq 0$) can be calculated from the solution of iteration i, using the recursive relation

$$\begin{aligned} A_1^i(\tau,z) &= -h(z+\tau) - \int_{-\infty}^{z} \{A_2^i(y,z)\}^* h(y+\tau)dy \\ A_2^{i+1}(\tau,z) &= -\int_{-\infty}^{z} \{A_1^i(y,z)\}^* h(y+\tau)dy \end{aligned} \tag{11}$$

where $A_{1,2}^i(\tau,z)$ are the two kernel functions of the ith iteration.

When the grating reflectivity is high, a large number of iterations is needed to accurately solve the GLM equation [14]. Furthermore, the accuracy of the iterative solution decreases as the distance along the grating increases, due to the increased effect of multiple reflections. Therefore, regions that are closer to the output end of the grating, require higher number of iterations than regions located at the beginning of the grating [14]. Theoretically, the iterative procedure converges and the error can be reduced as needed [8]. In practice, the reflection spectrum is presented using a finite bandwidth and resolution that prevent an accurate calculation of high-order iterations. Therefore, in highly reflecting gratings, the error of the iterative algorithm does not vanish when the number of iterations is increased. In

order to reduce the error in calculating high-order iterations, the time resolution should be increased. Therefore, the reconstruction of highly reflecting gratings requires a very high time resolution that dramatically increases the complexity of the solution.

III. The ILP Algorithm

In this section, we describe a new algorithm for solving the inverse scattering problem in fiber Bragg gratings. The algorithm, that will be referred to as the ILP, is a layer-peeling algorithm that is based on a solution to the GLM integral equation [(7)]. The ILP algorithm enables to solve numerically difficult inverse scattering problems, where previous algorithms failed to give an accurate result. Using the ILP algorithm, we could accurately solve the inverse scattering problem for gratings with a very high reflectivity, up to $1-10^{-10}$. The complexity of the ILP algorithm is on the same order as former layer-peeling algorithms. When a slight inaccuracy is allowed, the complexity of the ILP algorithm can be reduced significantly below the complexity of previously published layer-peeling algorithms.

The ILP algorithm is based on an iterative solution to the GLM equation combined with a layer-peeling procedure. The grating is divided into several layers that may have a nonuniform profile. A solution to the GLM equation is used to calculate the reflection coefficient of each layer in the grating from the reflection coefficient of the preceding layer. The solution to the GLM equation in each layer is also used to extract the profile of the layer. The procedure is repeated until the entire grating structure is revealed. The solution to the GLM equation for each layer is found using the iterative algorithm described in the previous chapter. Since we need to solve the GLM equation for a narrow layer only, a small number of iterations is all that is needed to obtain accurate results. Therefore, the complexity of the ILP algorithm remains on the same order as previously published layer-peeling algorithms. The calculation of the reflection coefficient of each layer is not based on the extracted profile of other layers in the grating. Therefore, inaccuracies in extracting the grating profile do not accumulate through the peeling procedure. A detailed description of our ILP algorithm is given below.

We define the local reflection coefficient $r(k,z) = u_1(k,z)/u_2(k,z)$, where $u_1(k,z)$ and $u_2(k,z)$ are the backward- and forward-propagating waves calculated for the boundary conditions $u_1(k,z=L)=0$ and $u_2(k,z=0)=1$. Since our problem is linear, $r(k,z)$ is equal to the reflection from the section of the grating located at the region $[z,L]$. The fields inside the grating are calculated by substituting (6) into (5), and are given in (12), shown at the bottom of the page. The local reflection coefficient is obtained from (12) as

$$r(k,z)=\exp(-2ikz)\frac{r(k)[1+\beta^*(k,z)]+\alpha(k,z)}{1+r(k)\alpha^*(k,z)+\beta(k,z)} \tag{13}$$

where

$$\alpha(k)=\int_{-\infty}^{2z} A_1(\tau-z,z)\exp(ik\tau)d\tau$$
$$\beta(k)=\int_{0}^{\infty} A_2(z-\tau,z)\exp(-ik\tau)d\tau. \tag{14}$$

Equation (13) is the basic equation of the ILP algorithm.

We divide the grating into M layers, each having a width of Δz. We define the local reflection coefficient of each layer $r_m(k) = r(k, m\Delta z)$, where $m = 0,1,\ldots,M-1$. The Fourier transform of the local reflection coefficient, $h_m(\tau) = 1/(2\pi)\int_{-\infty}^{\infty} r_m(k)\exp(-ik\tau)dk$, gives the impulse response of the grating section located at the region $[m\Delta z, L]$. The propagation of the local reflection coefficient along the grating is obtained from (13)

$$r_{m+1}(k)=\exp(-2ik\Delta z)\frac{r_m(k)[1+\beta_m^*(k)]+\alpha_m(k)}{1+r_m(k)\alpha_m^*(k)+\beta_m(k)} \tag{15}$$

where

$$\alpha_m(k)=\int_{-\infty}^{2\Delta z} A_{1,m}(\tau-\Delta z,\Delta z)\exp(ik\tau)d\tau$$
$$\beta_m(k)=\int_{0}^{\infty} A_{2,m}(\Delta z-\tau,\Delta z)\exp(-ik\tau)d\tau. \tag{16}$$

The kernel functions $A_{1,m}(\tau,z)$ and $A_{2,m}(\tau,z)$ are the solutions to (7) obtained by substituting the local impulse response $h_m(\tau)$, instead of the impulse response $h(\tau)$. Equation (15) gives the exact recursive connection between the reflection coefficients of successive layers.

The grating structure of the mth layer is extracted from the solution to the GLM equation using (8)

$$q(m\Delta z+z')=2A_{1,m}(z',z') \qquad 0\le z'\le \Delta z. \tag{17}$$

Note that the extracted grating structure is not used to propagate the reflection coefficient in (15). Therefore, the error in evaluating the grating profile does not accumulate along the grating.

When the width of each layer Δz is short enough, the Born approximation, given in (9), can be accurately used. Substituting (9) into (15) and (16), we obtain a simple equation for propagating the complex reflection coefficient along the grating

$$r_{m+1}(k)=\exp(-2ik\Delta z)\frac{r_m(k)-\overline{r}_m(k)}{1-r_m(k)\overline{r}_m^*(k)} \tag{18}$$

where

$$\overline{r}_m(k)=\int_{-\infty}^{2\Delta z} h_m(\tau)\exp(ik\tau)d\tau. \tag{19}$$

Equation (18) is the Born approximation to (15). The grating profile is extracted using the connection

$$q(m\Delta z+z')=-2h_m(2z'), \qquad 0\le z'\le \Delta z. \tag{20}$$

$$\begin{bmatrix} u_1(k,z)\\ u_2(k,z)\end{bmatrix}=\begin{bmatrix} r(k)\exp(-ikz)+\int_{-\infty}^{z}A_1(\tau,z)\exp(ik\tau)d\tau + r(k)\int_{-\infty}^{z}A_2^*(\tau,z)\exp(-ik\tau)d\tau\\ \exp(ikz)+\int_{-\infty}^{z}A_2(\tau,z)\exp(ik\tau)d\tau + r(k)\int_{-\infty}^{z}A_1^*(\tau,z)\exp(-ik\tau)d\tau\end{bmatrix}. \tag{12}$$

Since the local impulse response $h_m(\tau)$ is a causal function, the lower limit of the integral in (19) can be theoretically replaced by 0. In practice, the function $h_m(\tau)$ is computed from the local reflection coefficient $r_m(k)$ using FFT. The numerically calculated impulse function $h_m(\tau)$ becomes inaccurate and noncausal due to the finite bandwidth and spectral resolution used to present the local reflection coefficient. Therefore, a lower limit of $-\infty$ is needed in order to accurately propagate the local reflection coefficient. The use the lower limit of $-\infty$ significantly decreases the error due to numerical inaccuracies such as Gibbs phenomenon.

Equation (18) resembles the equation, that was used to propagate the reflection coefficient in the FDLP algorithm [11]. However, in [11], a constant number, that does not depend on the frequency, was used instead of the frequency-dependent function $\overline{r}_m(k)$ used in (18). Therefore, our solution is more general and more accurate than the solution used in [11]. We note that even in the case when each layer in the ILP algorithm contains only a single point, the function $\overline{r}_m(k)$ depends on the frequency since the lower limit in (19) is taken to be $-\infty$.

IV. Complexity and Numerical Implementation

In this section, we discuss the numerical implementation and the complexity of the ILP algorithm. As explained in the previous section, we need to solve the GLM equation for each layer in the grating, using the iterative procedure described in Section II. When the iterative solution to the GLM equation is implemented directly, the complexity of the solution for each iteration is equal to $O(N^3)$ [9], where N is the number of points in the grating spectrum. We use a new implementation of the iterative solution to the GLM equation, that reduces the complexity of the calculations to $O(N^2\log(N))$. The implementation is based on using FFT in the calculations of the integrals in (11).

The integrals in (11) can be calculated using the connection

$$\int_{-\infty}^{z} A^i_{1,2}(y,z)h(y+\tau)dy = \int_{-\infty}^{\infty} G^i_{1,2}(\tau-y,z)h(y)dy \quad (21)$$

where

$$G^i_{1,2}(\tau,z) = \begin{cases} A^i_{1,2}(-\tau,z), & \tau > -z \\ 0, & \text{otherwise.} \end{cases} \quad (22)$$

$A^i_j(\tau,z)$ are the kernel functions of the ith iteration ($j = 1, 2$). Since each of the two integrals in (21) is a convolution of two functions, $h(\tau)$ and $G^i_{1,2}(\tau,z)$, the integrals can be calculated in the frequency domain using FFT. Using (11) and (21), the complexity of calculating the kernel functions $\mathbf{A}(\tau,z)$ for a given value of z is $O(\ell N\log(N))$, where $\ell \geq 0$ is the number of iterations. The number of iterations significantly affects the computation time. Therefore, we choose to emphasize the effect of the number of iterations by adding it to the complexity calculations. Using (8) to calculate the grating profile, the total complexity needed to extract the grating profile is reduced to $O(\ell N^2\log(N) + N\log(N))$. The last term in the complexity expression gives the complexity of Born approximation ($\ell = 0$).

In our implementation of the ILP algorithm, we solve the GLM equation for each layer using FFT as described above. Since the length of each layer is short, only a limited number of iterations is needed to obtain an accurate result. We divide the grating into M layers; each contains $N/2M$ points of the grating profile. We note that although the spectrum contains N points, the profile of the whole grating contains only $N/2$ points, due to the casuality of the solution. The complexity of propagating the reflection coefficient from one layer to another using (11), (15), and (16) is equal to $O(\ell N\log(N)+N\log(N))$. The complexity of calculating the profile of a single layer using (11) and (17) is equal to $O(\ell(N/M)^2\log(N/M)+N\log(N))$. Since the grating profile is calculated for M layers, the overall complexity of extracting the whole grating structure is equal to $O(\ell(N)^2/M\log(N) + (\ell+1)NM\log(N))$. When Born approximation ($\ell = 0$) can be used to solve the GLM equation, the complexity of the ILP algorithm reduces to $O(NM\log(N))$.

The most accurate result in reconstructing the grating is obtained when the length of each layer in the ILP algorithm is minimal. In this case, each layer contains one point, and therefore the number of layers equals $M = N/2$. When each layer contains only one point, Born approximation should be used and the complexity of the solution is equal to $O(N^2\log(N))$. In a case where a slight decrease in the accuracy is acceptable, wider layers can be used, resulting in fewer layers. By decreasing the number of layers, the total complexity can be reduced below $O(N^2\log(N))$. When the length of the layers is increased, the use of the Born approximation may cause errors. The accuracy of the solution may be improved in this case by increasing the number of iterations used to solve the GLM equation. Although the use of a higher number of iterations requires more calculations, the total complexity can still be significantly reduced below $O(N^2\log(N))$, as is demonstrated in the next section. Therefore, by reducing the number of layers, we can significantly decrease the complexity of the ILP algorithm below that obtained by previously published layer-peeling algorithms.

The use of the ILP algorithm enables to overcome numerical problems that limit previous inverse scattering algorithms. The profile of the grating in a layer-peeling algorithm is obtained from the local impulse response $h_m(t)$, calculated by performing FFT on the local reflection coefficient $r_m(k)$. Since the bandwidth and the resolution of the local reflection coefficient $r_m(k)$ are limited, the calculated impulse response becomes inaccurate. In order to reduce the error, the spectral resolution should be high enough to avoid aliasing effect in the time domain [16]. Since the impulse response is a rapidly decaying function, a high enough spectral resolution can be practically chosen. The limited spectral bandwidth used to present the reflection coefficient posses a more difficult problem. When the reflectivity of the grating is high, an extremely broad spectrum is required in order to avoid a significant error when using former inverse scattering algorithms [8]–[11]. When the grating profile is reconstructed from measurements, the bandwidth is limited by experimental setup. When the grating is synthesized, the bandwidth is limited by calculation time. The limited bandwidth causes numerical errors, such as the Gibbs phenomenon, at the front edge of the impulse response [16]. Since the grating profile is extracted from the front edge of the impulse response, a large error is caused by the Gibbs phenomenon. Moreover, the error in extracting the grating profile accumulates in former

layer-peeling algorithms ([9]–[11]) through the propagation of the reflection coefficient. Since numerical errors, caused by insufficient bandwidth, do not rapidly accumulate in the ILP algorithm, the total error in reconstructing the grating is significantly reduced. Therefore, our algorithm can be used to analyze highly reflecting gratings with a narrower spectral bandwidth. Moreover, unlike in previously published layer-peeling algorithms, the Gibbs phenomenon can be further reduced in the ILP algorithm. The profile of each layer in the ILP algorithm is extracted by solving the GLM equation. The solution to the GLM equation for a given layer can be used to accurately extract the structure of nearby layers. The error in calculating the profile of one layer from the solution to the GLM equation in a nearby layer can be significantly lower than the error caused by the Gibbs phenomenon. Mathematically, when the Born approximation is used, the profile of the mth layer is calculated from the impulse response of layer $m-j$ using (10)

$$q[m\Delta z + z'] = -2h_{m-j}[2(j\Delta z + z')] \qquad 0 \le z' \le \Delta z. \tag{23}$$

Equation (23) enables to extract the profile of the grating from parts of the impulse response that are less affected by the Gibbs phenomenon. This procedure, that could not be implemented in previous layer-peeling methods, enables to reduce the ripples in the extracted profile.

V. Numerical Results

In this section, we demonstrate the use of the ILP algorithm for reconstructing highly reflecting fiber Bragg gratings. We compared the results of the ILP algorithm to the results of two DLP algorithms: FDLP [11] and FTDLP [9], as well as to an iterative solution to the GLM equation [8]. The ILP algorithm was found to be more accurate than the former algorithms when implemented with the same bandwidth and spectral resolution. When the reflectivity of the grating was not very high, the previous layer-peeling algorithms gave an accurate result. However, when the grating reflectivity was very high, only the ILP algorithm enabled to solve the numerically difficult inverse scattering problem. The complexity of the ILP algorithm was found to be similar or lower than the complexity of the most efficient inverse scattering algorithm-FDLP algorithm, described in [11]. When a small error in the result was acceptable, the complexity of the ILP algorithm was reduced below that of the DLP algorithms.

In the first example, shown in Fig. 1, we demonstrate the high accuracy of the ILP algorithm compared to previously published inverse scattering algorithms. The grating that was analyzed had a uniform profile with a refractive index modulation amplitude $n_1 = 6.5 \times 10^{-4}$ and a length of 4 mm. The spectral bandwidth of the grating reflection was 0.8 nm, and the maximum reflectivity was equal to 99.99%. The reflection coefficient of the grating was calculated using an implicit expression [1], [2] and was sampled over a bandwidth of 40 nm with a spectral resolution of 0.01 nm. The central wavelength of all the gratings analyzed in this paper is equal to $\lambda = 2n_{\text{avg}}\Lambda = 1550$ nm.

Each layer in the implementation of the ILP algorithm contained one point, and therefore the Born approximation could be accurately used to propagate the reflection coefficient [(18)]. After calculating the local reflection coefficient of each layer in the grating, the profile of the grating was extracted using (23) with $j = 3$. A Hanning window was used in the calculation of the grating profile from the reflection coefficient [(23)]. The window was used to reduce the ripples along the grating, caused by the abrupt change at the boundaries of the uniform grating. We note that the window was used only in the extraction of the grating profile, and not for propagating the reflection coefficient. Therefore, an error that may be caused by the smoothing operation of the window does not accumulate along the grating. Such a filter can not be used in conventional layer-peeling algorithms, since the filter affects the propagation of the reflection coefficient.

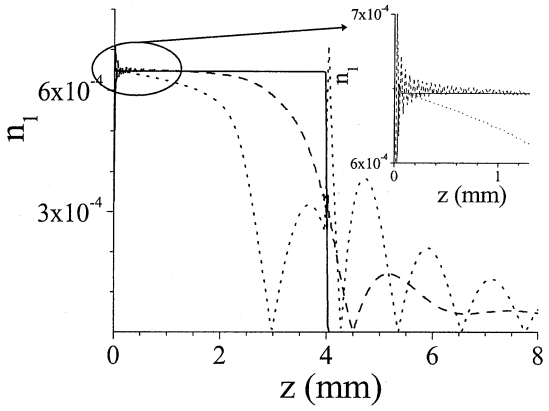

Fig. 1. Reconstructed modulation index $n_1(z)$ of a uniform grating with a refractive index modulation amplitude $n_1 = 6.5 \times 10^{-4}$, a length of 4 mm, and a maximum reflectivity of 99.99%, calculated using the ILP algorithm (solid line), the FDLP algorithm (dashed line), and iterative solution to the GLM equation with 70 iterations (dotted line). The reflection spectrum was sampled over a bandwidth of 40 nm with a resolution of 0.01 nm. The figure shows that an excellent reconstruction of the grating was obtained using the ILP algorithm, while the FDLP algorithm and the iterative solution to the GLM equation gave a large error. The inset of the figure shows a zoom on the profile close to the input end of the grating.

Fig. 1 compares the reconstructed profile of the grating, calculated using the ILP algorithm, the FDLP algorithm [11], and the iterative solution to the GLM equation [8]. The iterative solution was implemented using 70 iterations. We have found that the error did not change significantly when the number of iterations was increased above 70, due to an insufficient spectral width used to present the spectrum. The results shown in Fig. 1 demonstrate that an excellent reconstruction of the uniform grating was obtained using the ILP algorithm. On the other hand, the FDLP algorithm as well as the iterative solution to the GLM equation gave a large error. The iterative solution to the GLM equation was the slowest algorithm, and gave the worst results. Similar performance of the iterative solution was obtained in [9] for a weaker grating. Therefore, we will not show in the next examples the results of the iterative solution to the GLM equation. The FDLP algorithm required an extremely broad spectrum of about 1000 nm in order to accurately reconstruct the highly reflecting grating, analyzed in Fig. 1. Such a huge bandwidth is not practical, and therefore the large error caused by the FDLP algorithm may not be avoided for such a highly reflecting uniform grating. We have

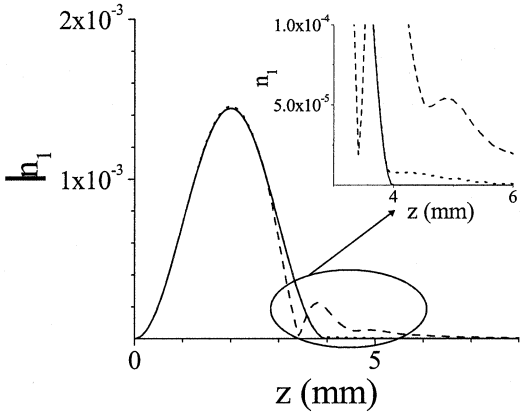

Fig. 2. Reconstructed modulation index $n_1(z)$ of a chirped raised cosine grating with a maximum refractive index modulation $n_1(z = 2\text{ mm}) = 1.45 \times 10^{-3}$, a length of 4 mm, and an average refractive index $n_0 = 0.25(4 \times 10^{-3} - z)$. The grating had a maximum reflectivity of 99.99%, a spectral bandwidth of about 1.7 nm, and a dispersion slope of 2.64 nm/cm. The reflection spectrum was sampled over a bandwidth of 15 nm with a resolution of 0.01 nm. The grating profile was extracted using the FTDLP algorithm [9] (dotted line), the FDLP algorithm [11] (dashed line), and the ILP algorithm (solid line). The inset of the figure shows a zoom on the profile near the output end of the grating.

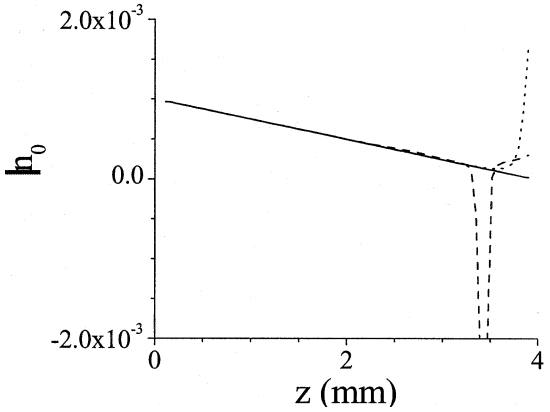

Fig. 3. Reconstructed average refractive index profile $n_0(z)$ of the chirped raised cosine grating shown in Fig. 2, calculated using the FTDLP algorithm (dotted line), the FDLP algorithm (dashed line), and the ILP algorithm (solid line). The reflection spectrum was sampled over a bandwidth of 15 nm with a resolution of 0.01 nm. Excellent reconstruction of the grating profile was obtained using the ILP algorithm, while a significant error was obtained in the result of both DLP algorithms.

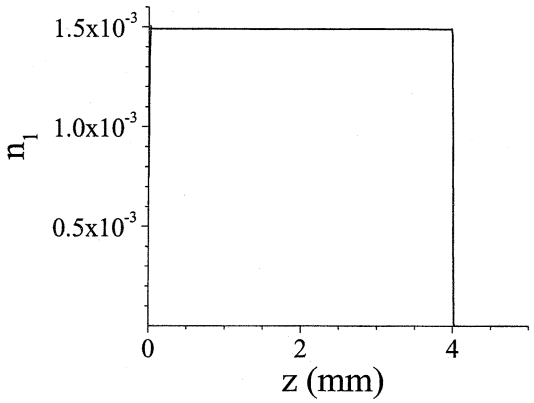

Fig. 4. Reconstructed modulation index $n_1(z)$ of a uniform grating with a refractive index modulation $n_1 = 1.5 \times 10^{-3}$, a length of 4 mm, and a maximum reflectivity of $1 - 10^{-10}$, calculated using the ILP algorithm. The reflection spectrum was sampled over a bandwidth of 80 nm with a resolution of 0.005 nm.

also reconstructed the grating using the FTDLP algorithm [9]. Although the FTDLP algorithm is usually more robust than the FDLP algorithm, in the particular example, shown in Fig. 1, the FTDLP gave a worse result than that obtained using the FDLP algorithm.

The reconstruction of a uniform grating is a numerically difficult task due to the abrupt change in the refractive index at the boundaries of the grating. In the next example, we show that even when the grating has a smooth profile, the ILP algorithm can give a more accurate result than obtained by both DLP algorithms. The grating that was analyzed had a chirped raised cosine profile with a length of 4 mm. The refractive index profile had a maximum amplitude of $n_1(z = 2\text{ mm}) = 1.45 \times 10^{-3}$. The average refractive index profile, that caused the chirp, was equal to $n_0(z) = 0.25(4 \times 10^{-3} - z)$. The grating had a maximum reflectivity of 99.99%, a spectral bandwidth of about 1.7 nm, and a dispersion slope of 2.64 nm/cm. Each layer in the ILP algorithm contained one point, and the GLM equation was solved using Born approximation [(18)–(20)]. Since the grating profile was smooth, we did not use a Hanning window to extract the grating profile as in the first example. The reflection spectrum was sampled over a bandwidth of 15 nm with a resolution of 0.01 nm. Figs. 2 and 3 show the profile of the grating amplitude, $n_1(z)$, and the average refractive index, $n_0(z)$, calculated using the FTDLP algorithm [9] (dotted line), the FDLP algorithm [11] (dashed line), and the ILP algorithm (solid line). The figures demonstrate again that an excellent reconstruction of the grating profile was obtained using the ILP algorithm. On the other hand, the result of both DLP algorithms contained a significant error especially in the reconstructed average refractive index of the grating, $n_0(z)$. The implementation of the FTDLP algorithm, gave a more accurate result than obtained using the FDLP algorithm. When the bandwidth of the reflection spectrum was greater than about 25 nm, the FTDLP algorithm gave an accurate result.

In order to further demonstrate the stability and the accuracy of the ILP algorithm, we reconstructed a uniform grating with a maximum reflectivity of $1 - 10^{-10} = 0.999\,999\,999\,9$. The grating had a uniform profile with a refractive index modulation amplitude of $n_1 = 1.5 \times 10^{-3}$ and length of 4 mm. The reflection coefficient was sampled over a bandwidth of 80 nm with a spectral resolution of 0.005 nm. The extraction of the grating profile was performed as in the first example. Fig. 4 shows the profile of the grating, reconstructed by the ILP algorithm. The figure demonstrates that an excellent reconstruction was obtained even for such a highly reflecting grating. The FDLP and the FTDLP algorithms as well as the iterative solution to the GLM equation could not reconstruct the highly reflecting grating using a practical bandwidth.

The ILP algorithm enables to accurately reconstruct highly reflecting gratings from a reflection coefficient sampled over a significantly narrower bandwidth than required by former DLP algorithms. This advantage of the ILP algorithm becomes especially important in reconstructing highly reflecting gratings

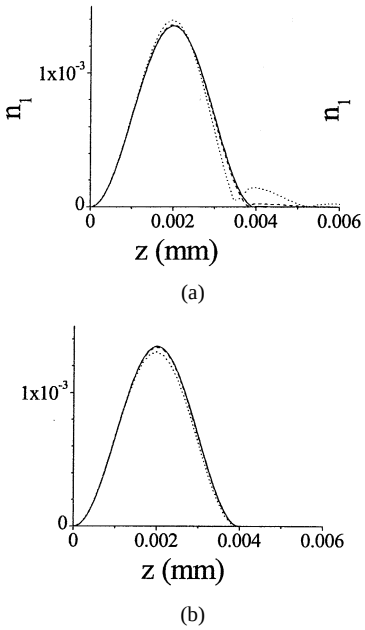

Fig. 5. Reconstructed modulation index, $n_1(z)$, of a raised cosine grating with a refractive index modulation $n_1 = 1.35 \times 10^{-3}$, a length of 4 mm, calculated using (a) the FDLP algorithm and (b) the ILP algorithm . The reflection spectrum was sampled over a bandwidth 20 nm (solid line), 10 nm (dashed line), and 5 nm (dotted line), with a resolution of 0.01 nm.

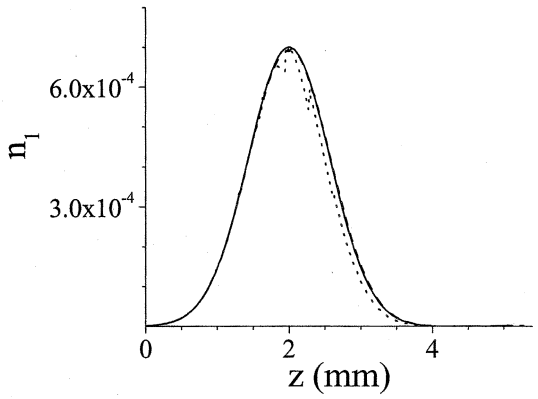

Fig. 6. Reconstructed modulation index profile $n_1(z)$ of a Gaussian grating with a maximum refractive index amplitude $n_1(z = 2 \text{ mm}) = 7 \times 10^{-4}$, a length of 4 mm, a full-width at half-maximum of 1.34 mm, and a maximum reflectivity of 93%. The grating was reconstructed using Born approximation (dotted line) and first-order approximation to the GLM equation (dashed line). The results are compared with exact grating profile (solid line). The reflection spectrum was sampled over a bandwidth of 40 nm with a resolution of 0.08 nm. The first-order approximation gave an accurate result with a complexity of $O(N^{3/2}\log(N))$.

from measurements. Fig. 5 shows the reconstructed modulation index $n_1(z)$ of a raised cosine grating with a refractive index modulation $n_1 = 1.35 \times 10^{-3}$, a length of 4 mm, and a spectral bandwidth of 1.4 nm, calculated using the FTDLP algorithm [9] and the ILP algorithm. The maximum reflectivity of the grating was equal to 99.99%. The reflection spectrum was sampled over a bandwidth of 20 nm (solid line), 10 nm (dashed line), and 5 nm (dotted line), with a resolution of 0.01 nm. The FDLP algorithm gave a larger error than obtained in the FTDLP algorithm, and therefore we did not include its results in the graph. Fig. 5 shows that a bandwidth of 5 nm was sufficient to obtain an accurate result using the ILP algorithm, while the FTDLP algorithm required a bandwidth of 20 nm.

The FTDLP algorithm is more complex and requires a longer runtime than the FDLP or the ILP algorithms. In the last example, we show that when a slight decrease in the accuracy of the calculation is acceptable, the complexity of the ILP algorithm can be reduced below that of the FDLP algorithm. The FDLP algorithm was considered in previous work as the most efficient inverse scattering algorithm [11]. The decrease in the complexity of the ILP algorithm was obtained by increasing the length of the layers, without significantly increasing the number of iterations required to accurately solve the GLM equation. The grating that was analyzed had a Gaussian profile with a maximum modulation amplitude, $n_1(z = 2 \text{ mm}) = 7 \times 10^{-4}$, a length of 4 mm, and a full-width at half-maximum of 1.34 mm. The maximum reflectivity of the grating was 93%. No chirp was added to the grating. The reflection spectrum was sampled over a bandwidth of 40 nm with a resolution of 0.08 nm. The number of points in the grating profile was equal to $N/2 = 250$. The grating was divided into 16($\approx N^{1/2}$) layers, and therefore the complexity of the solution was equal to $O(N^{3/2}\log(N))$. Fig. 6 shows the reconstructed profile obtained using Born approximation (dotted line) and using a first-order iteration (dashed line). The results are compared to the known grating profile (solid curve). The figure shows that an accurate reconstruction of the grating was obtained when first-order iterative solution to the GLM equation was used. Therefore the complexity of the solution was equal to $O(N^{3/2}\log(N))$, compared to a complexity of $O(N^2)$, needed in the FDLP algorithm. Indeed, the runtime of the ILP algorithm was about half of the runtime of the FDLP algorithm. The difference between the runtimes is smaller than can be expected by comparing the complexity of the two algorithms. Since the computer code of the ILP algorithm is more complicated than the code of the FDLP algorithm, we expect that the difference between the runtime of the two algorithms can be significantly increased by optimizing the code of the ILP algorithm.

VI. Conclusions

We have demonstrated a new inverse scattering method for reconstructing highly reflecting fiber Bragg gratings. The method, ILP, is based on solving the GLM integral equation in a layer-peeling procedure. Unlike in previously published layer-peeling algorithms, the structure of each layer in the ILP algorithm can have a nonuniform profile. Moreover, errors due to the limited bandwidth used to sample the reflection coefficient, do not rapidly accumulate along the grating. Therefore, the error in the new algorithm is smaller than in previous layer peeling algorithms. The integral layer-peeling algorithm was compared to two DLP algorithms and to an iterative solution to the GLM equation. The comparison indicates that the ILP algorithm enables to solve numerically difficult inverse scattering problems, such as to reconstruct gratings with a very high reflectivity, where previous algorithms failed to give an accurate result. The complexity of the ILP algorithm is on the same order as in previous peeling algorithms. When a small error is acceptable, the complexity of the ILP algorithm could be significantly reduced below the complexity of previously published layer-peeling algorithms.

REFERENCES

[1] H. Kogelnik, "Coupled wave theory for thick hologram gratings," *Bell Sys. Tech. J.*, vol. 48, pp. 2909–2947, Nov. 1969.

[2] T. Erdogan, "Fiber grating spectra," *J. Lightwave Technol.*, vol. 15, pp. 1277–1294, Aug. 1997.

[3] S. Keren and M. Horowitz, "Interrogation of fiber gratings by use of low-coherence spectral interferometry of noiselike pulses," *Opt. Lett.*, vol. 26, pp. 328–330, Mar. 2001.

[4] S. Keren, A. Rosenthal, and M. Horowitz, "Measuring the structure of highly reflecting fiber Bragg gratings," *IEEE Photon. Technol. Lett.*, vol. 15, pp. 575–577, Apr. 2003.

[5] G. H. Song and S. Y. Shin, "Design of corrugated waveguide filters by the Gel'fan-Levitan-Marchenko inverse scattering method," *J. Opt. Soc. Amer. A*, vol. 2, pp. 1905–1915, Nov. 1985.

[6] P. V. Frangos and D. L. Jaggard, "A numerical solution to the Zakharov-Shabat inverse scattering problem," *IEEE Trans. Antennas Propagat.*, vol. 39, pp. 74–79, 1991.

[7] ——, "Inverse scattering: Solution of coupled Gel'fand-Levitan-Marchenko integral equations using successive kernel approximation," *IEEE Trans. Antennas Propagat.*, vol. 43, pp. 547–552, 1995.

[8] E. Peral, J. Capmany, and J. Marti, "Iterative solution to the Gel'fan-Levitan-Marchenko coupled equations," *IEEE J. Quantum Electron.*, vol. 32, pp. 2078–2084, Dec. 1996.

[9] R. Feced, M. N. Zervas, and M. A. Muriel, "An efficient inverse scattering algorithm for the design of nonuniform fiber Bragg gratings," *IEEE J. Quantum Electron.*, vol. 35, pp. 1105–1115, Aug. 1999.

[10] L. Poladian, "Simple grating synthesis algorithm," *Opt. Lett.*, vol. 25, pp. 787–789, June 2000.

[11] J. Skaar, L. Wang, and T. Erdogan, "On the synthesis of fiber Bragg gratings by layer peeling," *J. Lightwave Technol.*, vol. 37, pp. 165–173, Feb. 2001.

[12] M. J. Ablowitz and H. Segur, *Solitons and the Inverse Transform*. Philadelphia, PA: SIAM, 1981.

[13] A. M. Bruckstein, B. C. Levy, and T. Kailath, "Differential methods in inverse scattering," *SIAM J. Appl. Math.*, vol. 45, no. 2, pp. 312–335, Apr. 1985.

[14] L. Poladian, "Iterative and noniterative design algorithms for Bragg gratings," *Opt. Fiber Technol.*, vol. 5, pp. 215–222, Apr. 1999.

[15] S. Barcelos, M. N. Zervas, R. I. Laming, D. N. Payne, L. Reekie, J. A. Tucknott, R. Kashyap, P. F. McKee, F. Sladen, and B. Wojciechowicz, "High accuracy dispersion measurement of chirped fiber gratings," *Electron. Lett.*, vol. 31, pp. 1280–1282, 1995.

[16] J. G. Proakis and D. G. Manolakis, *Digital Signal Processing: Principles, Algorithms, and Applications*, 3rd ed. London, U.K.: Prentice-Hall International, 1996.

Amir Rosenthal was born in Haifa, Israel, in 1981. He received the B.Sc. degree in electrical engineering (with high honors) in 2002 from The Technion—Israel Institute of Technology, Haifa, where he is currently working toward the M.Sc. degree in electrical engineering.

His research interests include synthesis and characterization of fiber gratings.

Mr. Rosenthal received a certificate of merit from the Education and Culture Committee of the Israeli Parliament in 2002.

Moshe Horowitz, photograph and biography not available at the time of publication.